164. Reinvestigation of the Conformation of Cyclosporin A in Chloroform

by **Horst Kessler***, **Matthias Köck**, **Thomas Wein**, and **Matthias Gehrke**

Organisch-Chemisches Institut der Technischen Universität München, Lichtenbergstr. 4, D-8046 Garching

(6. VIII. 90)

New investigations of cyclosporin A in $CDCl_3$ have been performed to obtain additional and more accurate distance restraints than utilized in our previous studies of cyclosporin A. Build-up rates at 600 MHz using 6 different mixing times at low temperatures (252.5 K) were determined and transformed into distances using the two-spin approximation. With the new distance restraints in the MD simulations using the GROMOS package, we can unambiguously conclude the presence of a βII'-turn. The new structure resembles the X-ray structure more than the structure previously determined, especially regarding the orientation of the MeBmt side chain. In the new structure and in the solid state, the side chain is folded over the backbone (although there are substantial differences in the χ_1 torsion), in contrast to the old structure, where the side chain is extended away from the backbone.

Some years ago, we studied the conformation of cyclosporin A in $CDCl_3$ by NMR spectroscopy [1–4]. In this study, 1D difference NOE effects as well as homo- and heteronuclear vicinal coupling constants [3] [5] were used as experimental data for the conformational analysis. These data were used in several conformational calculations such as distance geometry [6], restrained molecular dynamics *in vacuo* as well as in solution (solvent CCl_4 and H_2O) [7] [8]. In addition, systematic-search force-field calculations [9] [10] and another calculation algorithm which scans the total conformational space better than conventional MD methods [11] were applied to this molecule.

Cyclosporin A, cyclo(-MeBmt^1-Abu^2-Sar^3-MeLeu^4-Val^5-MeLeu^6-Ala^7-D-Ala^8-MeLeu^9-MeLeu^{10}-MeVal^{11}-) [12] [13], is a neutral, cyclic undecapeptide with seven *N*-methylated amino acids, containing only lipophilic amino acids. It was isolated in 1976, together with cyclosporin C [14], from the fungus species *Tolypocladium inflatum* GAMS [15]. Cyclosporin A is today a well known drug (since 1983 it is known by the trade name *Sandimmune*®) to prevent graft rejection in organ transplants. The first use of cyclosporin A during transplantation was in 1978 [16]. Many different synthetical and natural cyclosporins have been tested, but cyclosporin A is still the most active one [17]. A detailed knowledge of the structure of cyclosporin A in solution under different environmental conditions is the basis for structure-activity relationships allowing the design of new derivatives with higher activity and less side effects. The first total synthesis of cyclosporin A was described by *Wenger* in 1984 [18] [19]; parts of the sequence were published earlier [20] [21]. The residue MeBmt (= (4*R*)-4-[(*E*)-but-2-enyl]-4,*N*-dimethyl-L-threonine = (2*S*,3*R*,4*R*,6*E*)-3-hydroxy-4-methyl-2-(methylamino)oct-6-enoic acid) plays a central role in the activity of the immunosuppressant. At the moment, MeBmt is of great synthetical interest [22–30].

Cyclosporin A in solvents of low polarity such as C_6D_6 [31] and (D_8)THF [32][1]) show no major conformational differences from that observed in $CDCl_3$. In solvents of higher polarity, changes in the backbone conformation are directly visible in the NMR spectra; many conformations are in equilibrium, interconverting slowly on the NMR time scale (*e.g.* in DMSO, at least seven conformations can be observed [4]). Cyclosporin A is insoluble in H_2O. Hence, an accurate structure in $CDCl_3$ would be the first step in understanding more about the structure-activity relationships of this important molecule.

In our first structure determination of cyclosporin A, we used 58 distance restraints which were achieved by measuring 1D NOE effects at 360 MHz and 300 K in the positive NOE regime (fast-motion limit). Under these conditions, it was possible to obtain only ranges of distances with low accuracy and maximum distances of *ca.* 300 to 350 ppm. One problem which could not be solved in the first structure determination was the unequivocal identification of the type of the β-turn: both the βI- and the βII′-turn were allowed solutions for the obtained distances [9] [10], although the MD results preferred a βII′-turn [7]. The X-ray structure of cyclosporin A was determined in 1985 [3]. This structure has an almost identical backbone conformation as found by NMR in the apolar solvent. However, there were distinct differences in the orientation of the side chains about χ_1, the most significant being the orientation of the MeBmt residue: In the crystal, the MeBmt side chain is folded over the backbone, whereas in solution, it extends out into the solvent. It was shown by energy calculations that conformations of cyclosporin A similar to the crystal structure are lower in energy than the conformation derived from the NMR study in $CDCl_3$ [33]. In contrast, calculations carried out for an aqueous solution show the same conformation on the MeBmt side chain as found in the crystal structure [8].

With these inconsistencies, we felt that more accurate distances are needed. We, therefore, set out to measure NOE effects under different conditions. Here, we report measurements of cyclosporin A in the slow-motion limit (negative NOE effects) in $CDCl_3$.

NMR Measurements. – No detectable NOE effects were obtained at room temperature and high magnetic fields [34]. The correlation time of cyclosporin A in chloroform at room temperature is *ca.* 0.5 ns [35]. To produce a longer correlation time and observable NOE effects, the temperature was reduced to 252.5 K. The measurements were carried out on a *Bruker AM 600* spectrometer to obtain sufficient resolution. The constant temperature was achieved with a cryostat using silicon oil as a coolant.

All ^{1}H-NMR chemical shifts were reassigned at this temperature by a DQF-H,H-COSY. As shown in *Table 1*, there are no major changes, apart from the NH protons when compared with the δ(H) measured at 296 K. However, there is another conformation visible besides the main conformation of cyclosporin A, interconverting slowly on the NOE time scale. It is highly probable that these two conformations are due to *cis/trans* isomerization about *N*-alkylated peptide bonds. As the population of the minor conformation is *ca.* 6%, we were not able to solve this structure. In the following, we will discuss only the major conformation. Six NOESY spectra with mixing times of 80, 120, 160, 200, 240, and 300 ms were recorded without zero-quantum suppression. In *Fig. 1*, the complete NOESY spectrum (600 MHz, $CDCl_3$, 252.5 K) of cyclosporin A is shown, and expanded portions (*Figs. 2* and *3*) illustrate some assignments and the quality of the spectrum.

[1]) The measuring temperature for NOESY spectra was 252.5 K and not 250 K as described in this paper.

Table 1. *^{1}H-NMR Chemical Shifts (δ) at 250 and 296 K.* In $CDCl_3$; the chemical shifts at 250 K were obtained from a 500-MHz DQF-H,H-COSY spectrum.

Residue No.	Amino acid	Group	δ [ppm]		Residue No.	Amino acid	Group	δ [ppm]	
			250 K[a])	296 K[b])				250 K[a])	296 K[b])
1	MeBmt	MeN	3.47	3.52	6	MeLeu	MeN	3.19	3.25[c])
		H–C(α)	5.42	5.45			H–C(α)	4.89	5.02
		H–C(β)	3.65	3.82			H–C(β)	2.07	2.06
		OH	4.30	3.87			H′–C(β)	1.25	1.41
		H–C(γ)	1.56	1.63			H–C(γ)	1.72	1.76
		Me–C(γ)	0.58	0.72			CH_3(δ)	0.89	0.94
		H–C(δ)	2.45	2.41			CH_3(δ')	0.76	0.85
		H′–C(δ)	1.52	1.73					
		H–C(ε)	5.28	5.36	7	Ala	NH	8.00	7.75
		H–(ζ)	5.35	5.35			H–C(α)	4.49	4.52
		Cl_3 (η)	1.60	1.62			CH_3(β)	1.30	1.36
2	Abu	NH	8.08	7.93	8	D-Ala	NH	7.17	7.18
		H–C(α)	4.98	5.03			H–C(α)	4.77	4.84
		H–C(β)	1.69	1.74			CH_3(β)	1.22	1.26
		H′–C(β)	1.55	1.60					
		CH_3(γ)	0.82	0.87	9	MeLeu	MeN	3.06	3.12[c])
							H–C(α)	5.63	5.70
3	Sar	MeN	3.32	3.40[c])			H–C(β)	2.17	2.13
		H–C(α)	4.70	4.76			H′–C(β)	1.11	1.25
		H′–C(α)	3.25	3.23			H–C(γ)	1.28	1.32
							CH_3(δ)	0.92	0.97
4	MeLeu	MeN	3.05	3.11[c])			CH_3(δ')	0.81	0.89
		H–C(α)	5.31	5.34					
		H–C(β)	1.93	2.00	10	MeLeu	MeN	2.63	2.70[c])
		H′–C(β)	1.62	1.64			H–C(α)	5.06	5.10
		H–C(γ)	1.35	1.44			H–C(β)	1.93	2.13
		CH_3(δ)	0.90	0.95			H′–C(β)	1.28	1.24
		CH_3(δ')	0.82	0.88			H–C(γ)	1.38	1.49
							CH_3(δ)	1.02	0.98
5	Val	NH	7.50	7.47			CH_3(δ')	0.95	0.98
		H–C(α)	4.62	4.67					
		H–C(β)	2.34	2.41	11	MeVal	MeN	2.66	2.71
		CH_3(γ)	1.00	1.06			H–C(α)	5.04	5.15
		CH_3(γ')	0.85	0.90			H–C(β)	2.11	2.17
							CH_3(γ)	0.99	1.01
							CH_3(γ')	0.81	0.87

[a]) Calibrated on the solvent signal (7.26 ppm), all data were obtained from a 4-K spectrum.
[b]) Calibrated on the internal standard TMS, all data were obtained from a 2-K spectrum.
[c]) 32-K data points.

We have seen no reason for using the zero-quantum suppression because the zero-quantum effects do not affect the integrals if the integration limits are defined big enough. The suppression of the zero-quantum effects, with the variation of mixing time or a π-pulse, lead to an increase of the t_1 noise because the zero-quantum effects will distribute through the whole ω_1 dimension. The integration of the cross-peaks were carried out with and without base-plane offset. In total, more than 500 cross-peaks were measured in the NOESY spectra. Cross-peaks from chemical exchange between the two conformations were excluded, based on comparison with a ROESY spectrum [36] [37] measured at 250 K. For some cross-peaks, the intensity on both sides of the diagonal could not be evaluated. This was especially true for the cross-peaks of the *N*-methyl groups, because of t_1 noise.

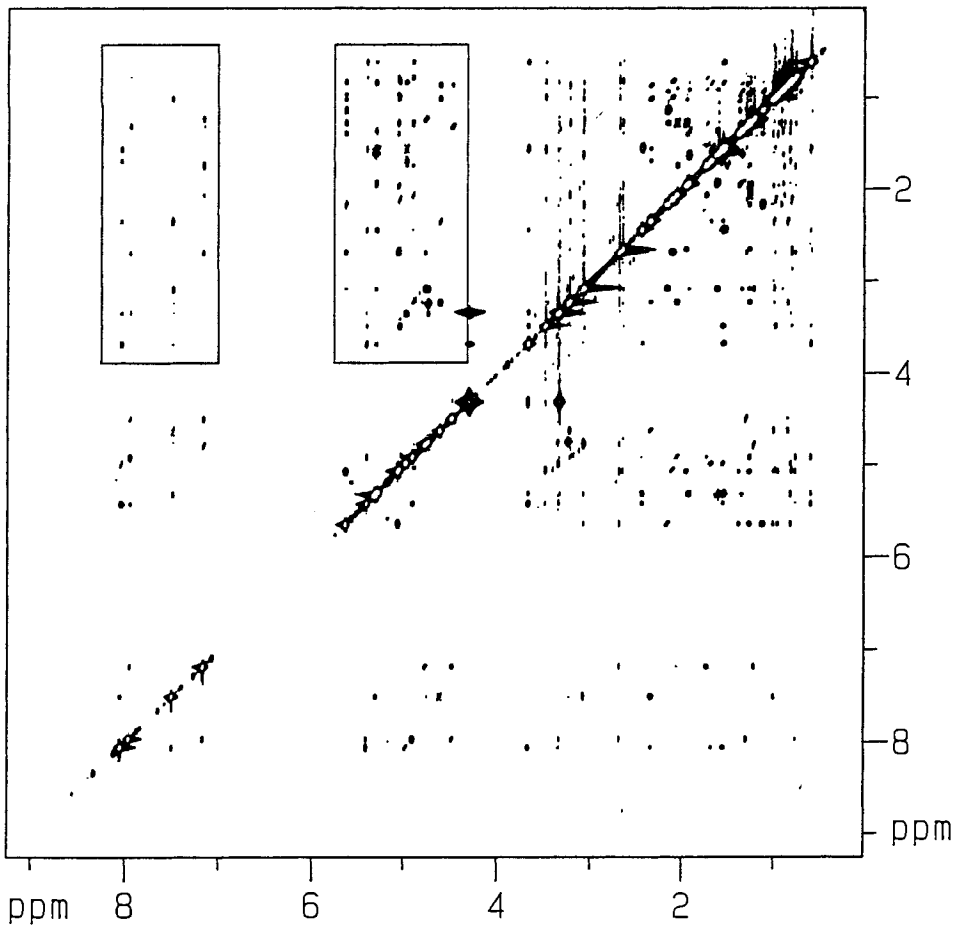

Fig. 1. *600-MHz NOESY spectrum of cyclosporin A at 252.5 K in $CDCl_3$ obtained with a mixing time of 200 ms.* The indicated areas are expanded in *Figs. 2* and *3*, the left one in *Fig. 2* and the right in *Fig. 3*.

The build-up of the NOE effects were calculated from the NOESY spectra with six different mixing times using an exponential fit[2]). The NOE data were evaluated under the assumption that the molecule is rigid and shows an isotropic overall molecular reorientation. It was also shown by model-independent [35] and model-dependent [3] analysis of the ^{13}C relaxation times, that the assumption of overall isotropic motion of cyclosporin A is appropriate. The two-spin approximation was used here. It has been shown and discussed often in the literature that the interconversion of cross-relaxation rates into distances using the two-spin approximation may result in significant systematic deviation from actual distances, especially for longer distances [38]. Currently, we are exploring the use of the iterative relaxation matrix approach (IRMA) [39] [40] to overcome these

[2]) The NMR program of the group of Prof. *Robert Kaptein*, Utrecht, was used on a *VAX-6210* computer.

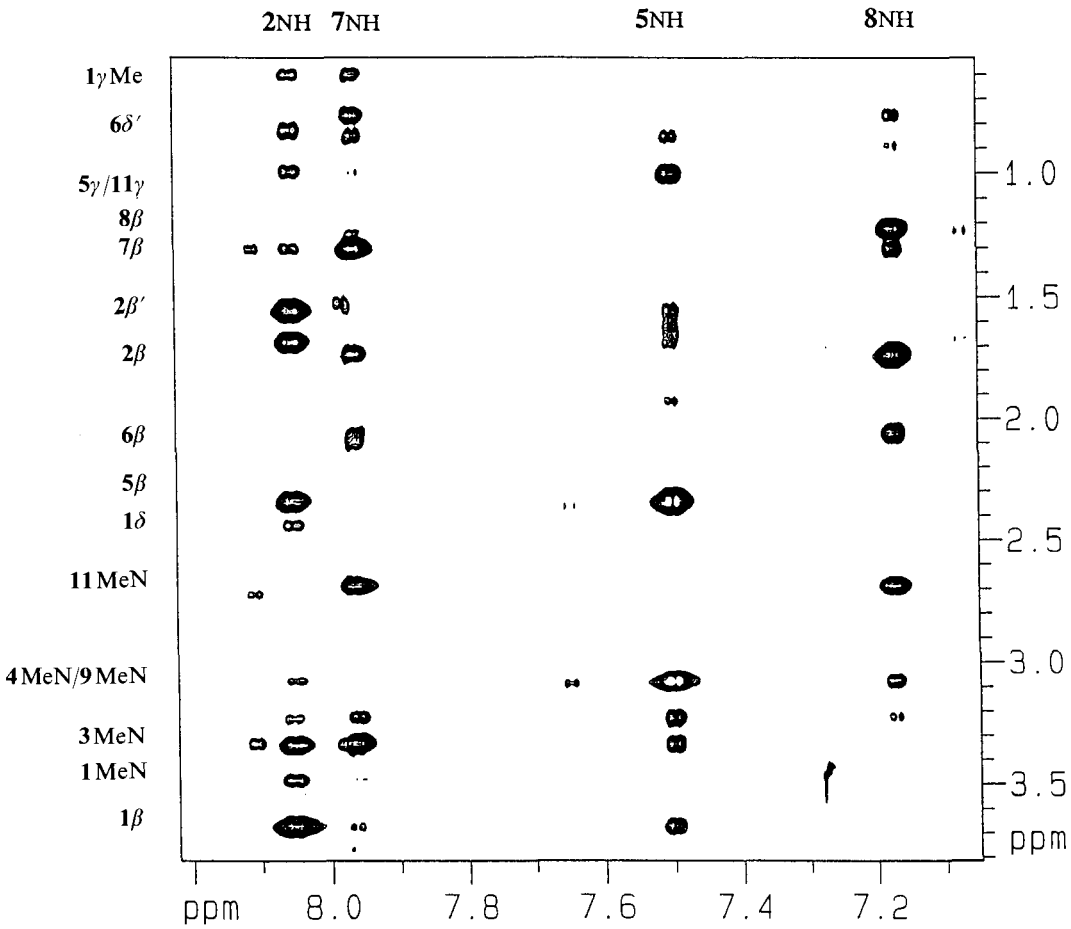

Fig. 2. *Expanded region of the spectrum of* Fig. 1 *in which the NH/β, γ, δ region is shown.* This region is essentially free of any zero-quantum effects. The assignments on the *y*-axis of the plots of *Figs. 2* and *3* are not complete, for a precise overview of the assignments, *Table 1* with all the chemical shifts can be used. Bold-type numbers refer to residue numbers.

problems. In *Table 2* all the distances obtained from the NOESY spectra and the distances after the MD simulations are shown.

Structure Refinement by Molecular-Dynamics (MD) Simulation. – The programs used for performing the MD calculations and the analysis of cyclosporin A were taken from the GROMOS (*gro*ningen *mo*lecular *s*imulation programs) program library [41]. For interactive modelling of the molecule, we used the program INSIGHT (BIOSYM). All calculations were performed on *Silicon Graphics 4D/240SX* and *4D/70GTB* computers.

Improved NMR techniques and the availability of 600-MHz spectrometers increased the number of constraints to 117 distances derived from NOE build-up rates (*Table 2*). We decided to take the structure MDS1 [7]

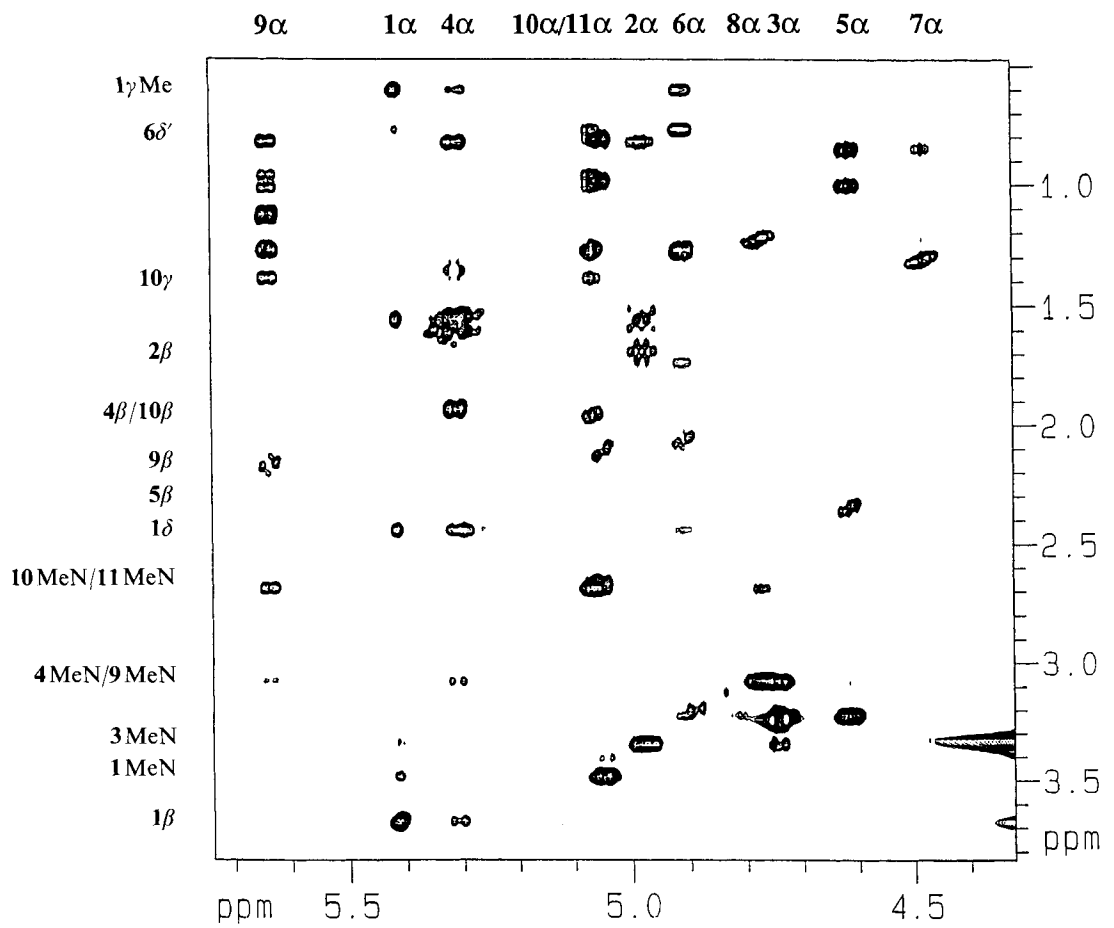

Fig. 3. *Expanded region of the spectrum of* Fig. 1 *in which the α/MeN, β, γ, δ region is shown.* In this part, several anti-phase peaks are visible because, no zero-quantum suppression was applied. Bold-type numbers refer to residue numbers.

(*Fig. 4*) which best fit 58 previously available experimental distance constraints as a starting structure for our new MD calculation. Unlike in our previous investigation, we have now taken the NOE between all four MeLeuC$H_2(\beta)$ proton paris for calibration and calculated the other distances from the NOE build-up rates. The MeLeuC$H_2(\beta)$ have similarNT_1 values as the C(α)'s [35], and the calibration with the Sar^{3}C$H_2(\alpha)$ leads to similar distances.

A harmonic restraint function was used for upper and lower boundaries, however, the distance-restraints function in the force field switches from harmonic to linear when the deviation is greater than 10% from the target distance. The upper bound distances are given in *Table 2*. For the lower bounds, 100 and 90 pm were subtracted for each Me and non-stereospecifically assigned CH_2 group, respectively. The χ_1 angle of Val^5 and MeVal^{11} were fixed to $-60°$ with a force constant of 100 kJ·mol^{-1} because of the large $J(H-C(\alpha), H-C(\beta)$ coupling constants (*i.e.* 10 and 11 Hz, resp.). In a MD run without an additional potential, these angles yielded a mean conformation with $\chi_1 = -149°$ for Val^5 and $\chi_1 = -153°$ for MeVal^{11} which is incompatible with the observed $J(H-C(\alpha), H-C(\beta))$. We have observed similar effects (possibly caused by vacuum effects or the overemphasize of some NOE's compared to others) previously and recommend a MD calculation with restrained side-chain conformation for the most populated rotamer according to J-coupling constants [5]. To ensure that the starting structure does not remain in a local minimum determined by the 58 distance constraints previously used, we heated up the system to 1000 K for

Table 2. *Experimental and Calculated Distances of Cyclosporin A*

Cross peaks (involved protons)		Distance [pm]		Cross peaks (involved protons)		Distance [pm]	
		from build-up rate	from 'MD'			from build-up rate	from 'MD'
MeBmt^1*Me*N	MeBmt^1*H*–C(α)	432	350	MeBmt^1*Me*–C(γ)	Abu^{2}N*H*	527	506
MeBmt^1*Me*N	MeBmt$^1H_{(pro\text{-}R)}$–C(δ)	415	292	MeBmt$^1H_{(pro\text{-}R)}$–C(δ)	Abu^{2}N*H*	415	519
MeBmt^1*Me*N	MeBmt$^1H_{(pro\text{-}S)}$–C(δ)	384	380	MeBmt$^1H'_{(pro\text{-}S)}$–C(δ)	Ala^{7}N*H*	523	594
MeBmt^1*Me*N	MeBmt^1*Me*–C(γ)	572	588	MeBmt$^1H_{(pro\text{-}R)}$–C(δ)	MeLeu^6*H*–C(α)	351	370
MeBmt^1*Me*N	Abu^{2}N*H*	479	508	MeBmt^{1}O*H*	MeBmt^1*C*O	280	253
MeBmt^1*Me*N	MeVal^{11}*H*–C(α)	301	233	Abu^{2}N*H*	Abu^2*H*–C(α)	311	292
MeBmt^1*Me*N	MeVal^{11}*H*–C(β)	441	480	Abu^{2}N*H*	Abu$^2H_{(pro\text{-}R)}$–C(β)	315	239
MeBmt^1*Me*N	MeVal$^{11}Me_{(pro\text{-}R)}$(γ)	431	509	Abu^{2}N*H*	Abu$^2H_{(pro\text{-}S)}$–C(β)	296	363
MeBmt^1*Me*N	MeVal$^{11}Me_{(pro\text{-}S)}$(γ′)	574	410	Abu^{2}N*H*	Sar^3*Me*N	450	454
MeBmt^1*H*–C(α)	MeBmt^1*H*–C(β)	233	262	Abu^{2}N*H*	Val^{5}N*H*	321	345
MeBmt^1*H*–C(α)	MeBmt^1*Me*–C(γ)	372	393	Abu^{2}N*H*	Val^5*H*–C(β)	317	326
MeBmt^1*H*–C(α)	MeBmt$^1H_{(pro\text{-}R)}$–C(δ)	311	302	Abu^{2}N*H*	MeLeu^6*H*–C(α)	357	375
MeBmt^1*H*–C(α)	MeBmt$^1H'_{(pro\text{-}S)}$–C(δ)	292	401	Abu^{2}N*H*	MeVal$^{11}Me_{(pro\text{-}R)}$(γ)	470	651
MeBmt^1*H*–C(α)	Abu^{2}N*H*	221	219	Abu^2*H*–C(α)	Abu$^2H_{(pro\text{-}R)}$–C(β)	285	301
MeBmt^1*H*–C(α)	Sar^3*Me*N	527	552	Abu^2*H*–C(α)	Abu$^2H_{(pro\text{-}S)}$–C(β)	280	253
MeBmt^1*H*–C(α)	MeLeu^6*H*–C(α)	269	253	Abu^2*H*–C(α)	Sar^3*Me*N	318	257
MeBmt^1*H*–C(α)	MeLeu$^6Me_{(pro\text{-}R)}$(δ)	460	395	Abu$^2H_{(pro\text{-}R)}$–C(β)	Val^5*H*–C(β)	298	275
MeBmt^1*H*–C(α)	Ala^{7}N*H*	300	305	Sar^3*Me*N	Sar$^3H_{(pro\text{-}S)}$–C(α)	356	369
MeBmt^1*H*–C(α)	Ala^7*H*–C(β)	517	495	Sar^3*Me*N	Val^{5}N*H*	411	492
MeBmt^1*H*–C(α)	MeVal^{11}*Me*N	519	509	Sar$^3H_{(pro\text{-}S)}$–C(α)	MeLeu^4*Me*N	283	254
MeBmt^1*H*–C(β)	MeBmt^1*Me*–C(γ)	387	262	Sar$^3H_{(pro\text{-}S)}$–C(α)	Val^{5}N*H*	336	355
MeBmt^1*H*–C(β)	MeBmt$^1H_{(pro\text{-}R)}$–C(δ)	320	375	MeLeu^4*Me*N	MeLeu^4*H*–C(α)	437	377
MeBmt^1*H*–C(β)	MeBmt$^1H_{(pro\text{-}S)}$–C(δ)	250	348	MeLeu^4*Me*N	MeLeu$^4H_{(pro\text{-}R)}$–C(β)	336	332
MeBmt^1*H*–C(β)	Abu^{2}N*H*	274	332	MeLeu^4*Me*N	Val$^5Me_{(pro\text{-}R)}$(γ)	421	616
MeBmt^1*H*–C(β)	Sar^3*Me*N	383	399	MeLeu^4*H*–C(α)	MeLeu$^4H_{(pro\text{-}S)}$–C(β)	249	299
MeBmt^1*H*–C(β)	Val^{5}N*H*	369	375	MeLeu^4*H*–C(α)	MeLeu^4*H*–C(γ)	315	176
MeBmt^1*H*–C(β)	MeLeu^6*H*–C(α)	432	450	MeLeu^4*H*–C(α)	MeLeu$^4Me_{(pro\text{-}S)}$(δ)	354	275
MeBmt^1*H*–C(β)	Ala^{7}N*H*	471	530	MeLeu^4*H*–C(α)	Val^{5}N*H*	297	288
MeBmt^1*Me*–C(γ)	MeBmt$^1H_{(pro\text{-}R)}$–C(δ)	459	383	Val^{5}N*H*	Val^5*H*–C(α)	296	292
MeBmt^1*Me*–C(γ)	Sar^3*Me*N	550	627	Val^{5}N*H*	Val^5*H*–C(β)	249	236
MeBmt^1*Me*–C(γ)	MeLeu^6*H*–C(α)	397	437	Val^{5}N*H*	Val$^5Me_{(pro\text{-}S)}$(γ)	386	443

Table 2 (cont.)

Cross peaks (involved protons)		Distance [pm]	
		from build-up rate	from 'MD'
Val^5NH	$Val^5Me_{(pro\text{-}R)}(\gamma')$	454	332
Val^5NH	$Sar^3H_{(pro\text{-}R)}$–C(α)	366	458
Val^5NH	$MeLeu^4MeN$	349	309
Val^5H–C(α)	Val^5H–C(β)	318	297
Val^5H–C(α)	$Val^5Me_{(pro\text{-}S)}(\gamma)$	371	306
Val^5H–C(α)	$Val^5Me_{(pro\text{-}R)}(\gamma')$	383	295
Val^5H–C(β)	$MeLeu^6MeN$	410	485
$Val^5Me_{(pro\text{-}R)}(\gamma')$	$MeLeu^6MeN$	447	519
$Val^5Me_{(pro\text{-}R)}(\gamma')$	Ala^7H–C(α)	427	599
$MeLeu^6MeN$	$MeLeu^6H_{(pro\text{-}S)}$–C(β)	333	290
$MeLeu^6MeN$	$MeLeu^6H'_{(pro\text{-}R)}$–C(β)	340	325
$MeLeu^6H$–C(α)	$MeLeu^6H_{(pro\text{-}S)}$–C(β)	301	299
$MeLeu^6H$–C(α)	$MeLeu^6H'_{(pro\text{-}R)}$–C(β)	275	127
$MeLeu^6H$–C(α)	$MeLeu^6H$–C(γ)	327	307
$MeLeu^6H$–C(α)	$MeLeu^6Me_{(pro\text{-}R)}(\delta)$	395	283
$MeLeu^6H$–C(α)	Ala^7NH	213	221
$MeLeu^6H$–C(α)	D–Ala^8NH	357	421
$MeLeu^6H_{(pro\text{-}S)}$–C(β)	$MeLeu^6H$–C(γ)	271	247
$MeLeu^6H_{(pro\text{-}S)}$–C(β)	$MeLeu^6Me_{(pro\text{-}S)}(\delta)$	411	290
$MeLeu^6H$–C(γ)	Ala^7NH	401	397
$MeLeu^6H$–C(γ)	D-Ala^8NH	275	273
$MeLeu^6Me_{(pro\text{-}R)}(\delta')$	Ala^7NH	445	425
$MeLeu^6Me_{(pro\text{-}R)}(\delta')$	D–Ala^8NH	477	471
Ala^7NH	Ala^7H–C(α)	297	280
Ala^7NH	Ala^7H–C(β)	358	261
Ala^7NH	D–Ala^8NH	284	357
Ala^7NH	$MeVal^{11}MeN$	394	413
Ala^7H–C(α)	D–Ala^8NH	292	254
Ala^7H–C(α)	D–Ala^8H–C(β)	470	491
Ala^7H–C(β)	D–Ala^8NH	443	436
D–Ala^8NH	D–Ala^8H–C(α)	284	288
D–Ala^8NH	D–Ala^8H–C(β)	344	271
D–Ala^8NH	$MeLeu^9MeN$	569	510
D–Ala^8NH	$MeVal^{11}MeN$	400	419
D–Ala^8H–C(α)	$MeLeu^9MeN$	283	247
D–Ala^8H–C(α)	$MeVal^{11}MeN$	399	410
$MeLeu^9MeN$	D–Ala^8H–C(β)	521	415
$MeLeu^9MeN$	$MeLeu^9H$–C(α)	471	369
$MeLeu^9MeN$	$MeLeu^9H_{(pro\text{-}R)}$–C(β)	347	317
$MeLeu^9H$–C(α)	$MeLeu^9H_{(pro\text{-}R)}$–C(β)	293	303
$MeLeu^9H$–C(α)	$MeLeu^9H_{(pro\text{-}S)}$–C(β)	249	254
$MeLeu^9H$–C(α)	$MeLeu^9H$–C(γ)	281	288
$MeLeu^9H$–C(α)	$MeLeu^9Me_{(pro\text{-}S)}(\delta)$	390	296
$MeLeu^9H$–C(α)	$MeLeu^{10}H$–C(α)	180	152
$MeLeu^9H$–C(α)	$MeLeu^{10}H_{(pro\text{-}R)}$–C(β)	361	316
$MeLeu^9H$–C(α)	$MeLeu^{10}H$–C(γ)	294	286
$MeLeu^9H$–C(α)	$MeVal^{11}MeN$	459	321
$MeLeu^9H_{(pro\text{-}R)}$–C(β)	$MeLeu^{10}H$–C(γ)	267	251
$MeLeu^9H_{(pro\text{-}S)}$–C(β)	$MeLeu^{10}H$–C(α)	384	347
$MeLeu^9H'_{(pro\text{-}S)}$–C(β)	$MeLeu^{10}H$–C(γ)	285	376
$MeLeu^{10}MeN$	$MeLeu^{10}H_{(pro\text{-}R)}$–C(β)	395	337
$MeLeu^{10}H$–C(α)	$MeLeu^{10}H_{(pro\text{-}R)}$–C(β)	282	265
$MeLeu^{10}H$–C(α)	$MeLeu^{10}H$–C(γ)	308	230
$MeLeu^{10}H$–C(α)	$MeVal^{11}MeN$	318	267
$MeVal^{11}MeN$	$MeVal^{11}H$–C(β)	310	284
$MeVal^{11}H$–C(α)	$MeVal^{11}H$–C(β)	297	295

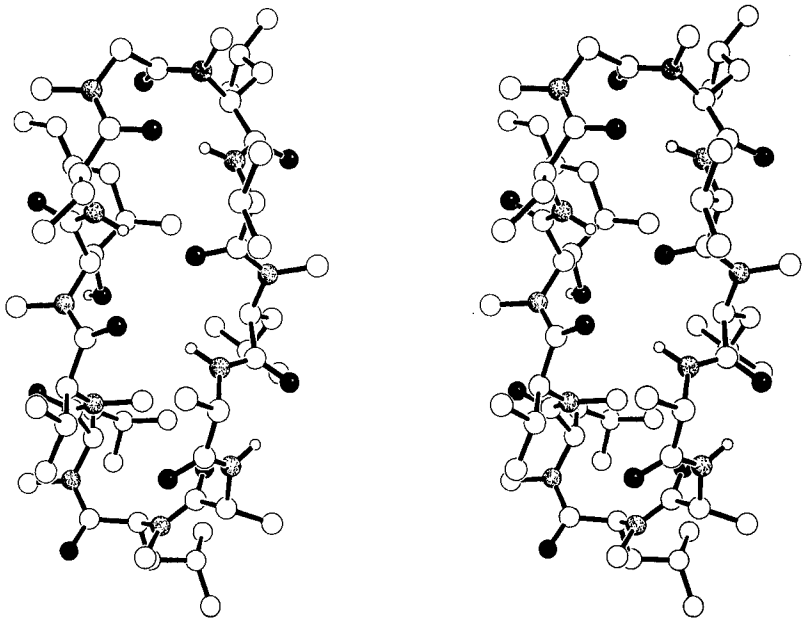

Fig. 4. *Stereo plot of the starting structure* (MDS1) *of MD calculation.* The βII′-turn between Abu^2 and Val^5 is oriented to the top. The O-atoms are filled and the N-atoms stipled.

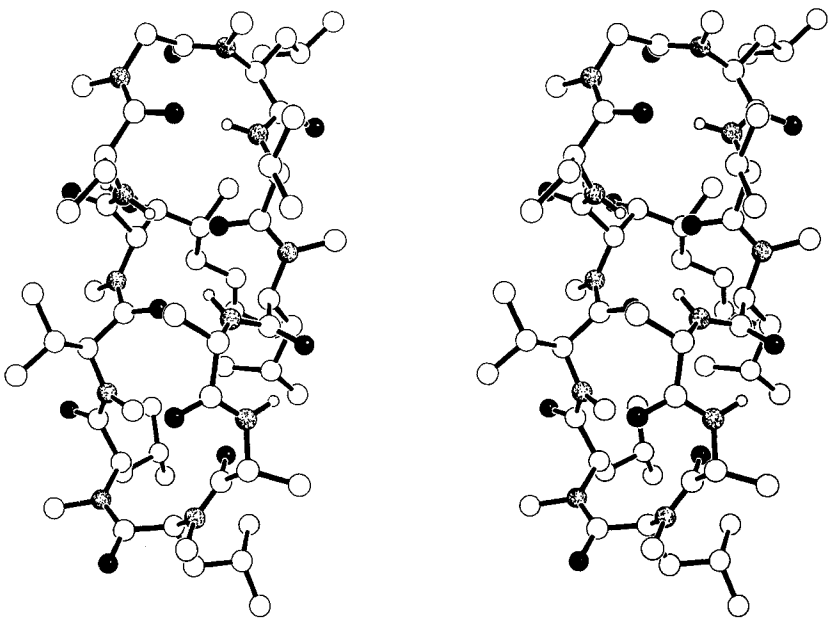

Fig. 5. *Stereo plot of the averaged MD structure* (MDNEW) *of cyclosporin A after restrained EM.* The βII′-turn between Abu^2 and Val^5 is oriented to the top. The O-atoms are filled in the N-atoms stipled.

2 ps by coupling the system to a thermal bath. During the next 3 ps, the temperature of the bath was reduced to 600 K. After these 5 ps of high-energy dynamics, the system was allowed to relax to 300 K in 5 ps. The structure was then minimized using the steepest descent algorithm (EM1). During these 10 ps of MD and the following EM, the force constant of the constraining potential for the NOE-derived distances was set to $K_{dc} = 4000$ kJ·mol^{-1}·nm^{-2}. In the first MD/EM cycle, only 77 distance constraints were used. After this, it was possible to increase the number of distance constraints to 118 because the ambiguities in the chemical-shift assignments of some protons could be removed by comparison with the EM1 structure. The intramolecular H-bridge between MeBmt^{1}O*H* and MeBmt^{1}C*O* which was derived by IR spectroscopy [3] and $J(H-C(\alpha), H-C(\beta))$ was used as an additional constraint. With the complete set of constraints, the MD/EM cycle was repeated. This was followed by 100 ps of MD with a lower force constant ($K_{dc} = 1000$ kJ·mol^{-1}·nm^{-2}, $T = 300$ K). The structure averaged over 10–110 ps was minimized again with the same K_{dc} as used in the final MD run. The initial structure (after 10 ps of high-temperature MD and EM) had the potential energy of 466 kJ·mol^{-1} in which the distance-restraints energy was the major part, 270 kJ·mol^{-1}. The minimized average structure had a potential energy of 173 kJ·mol^{-1} including 25 kJ·mol^{-1} of distance-restraints energy. This latter structure is shown in *Fig. 5*. The dihedral-restraint energy was less than 1 kJ·mol^{-1} in all structures.

The same cycle of 5 ps heated MD, 5 ps relaxation, first EM, 10–70 ps MD, and following EM was repeated with a starting structure similar to MDS2 but with a βI-turn manually inserted between Abu^{2}CO and Val^{5}N*H*. After 2 ps of heated MD, the turn had already flipped to the βII′-type.

In our first investigation of the structure of cyclosporin A which was based on 58 distance constraints (MDS1) [7], it turned out that the MeBmt side chain exhibits an extended conformation. To our surprise, in the new structure calculated with 118 distance constraints (MDNEW), the MeBmt side chain is folded over the backbone similar to the conformation observed in the X-ray structure. However, this was due to a change in χ_2 rather than χ_1 (*Table 3*). As a test of our constraints, we fixed the dihedral angles of the

Table 3. *Side-Chain Dihedral Angles* [°] *of Different Structures of Cyclosporin A*[a])

Residue		X-Ray	MDS1	MDNEW
MeBmt^1	χ_1	−166	−67 (9.7)	−77 (2.8)
	χ_2	74	163 (15.2)	91 (2.7)
	χ_3	−179	−119 (37.6)	−180 (3.8)
	χ_4	−126	175 (54.0)	168 (17.1)
	χ_5	−175	180 (8.1)	−180 (2.3)
Abu^2	χ_1	−178	−125 (50.1)	−70 (4.2)
MeLeu^4	χ_1	−51	−79 (16.8)	−151 (13.3)
	χ_2	−54	−80 (22.7)	−172 (4.6)
Val^5	χ_1	−51	−63 (10.3)	−61 (2.5)
MeLeu^6	χ_1	−176	−173 (14.0)	−178 (2.3)
	χ_2	−177	−133 (30.4)	−175 (2.7)
MeLeu^9	χ_1	−54	−72 (14.8)	−60 (2.6)
	χ_2	−63	−96 (34.3)	−70 (3.7)
MeLeu^{10}	χ_1	−163	−118 (35.7)	−148 (9.5)
	χ_2	−169	−80 (13.5)	−78 (6.3)
MeVal^{11}	χ_1	−53	−60 (8.9)	−60 (2.4)

[a]) Values in brackets denote the rms fluctuation obtained by averaging.

MeBmt side chain to the values reported for the MDS1 structure [7]. The consequence of this forcing potential was that the total potential energy increased dramatically and the constraints showed a greater violation than those observed in the MD runs in which the MeBmt dihedral angles were not fixed (see structure of cyclosporin A for details). Hence, we decided not to fix the dihedral angles of the MeBmt side chain. Only the χ_1 angle of MeBmt^1 was lightly fixed by the distance restraints from MeBmt^{1}O*H* to MeBmt^{1}C*O*. However, as the number of distance restraints which involve the MeBmt^1 side chain had increased to 25 in the present structural refinement, this guaranteed a good description of the conformation of the side chain.

Results of the Calculations. – The restrained MD calculations (see above) were performed to calculate the most populated structure of cyclosporin A in apolar solution. The resulting conformation of cyclosporin A is shown in *Fig. 5*. The *cis*-amide bond between MeLeu^9 and MeLeu^{10} is confirmed by the strong H–C(α)/H–C(α) NOE between these two residues. All N*H*'s are involved in internal H-bonds, with Val^{5}N*H* and Ala^{7}N*H* partially participating in three-center H-bonds (*Table 4*). The occurrence of the

Table 4. *Three-Center H-Bonds in Cyclosporin A from MDNEW.* d in pm, θ in °.

Donor (D)	Acceptor 1 (A1)	Acceptor 2 (A2)	d(H,A1)	d(H,A2)	d(D,A1)	d(D,A2)	θ(1)	θ(2)	%
Val^{5}N*H*	Abu^2*O*	Sar^3*O*	227	275	313	342	145	125	*2.1*
Ala^{7}N*H*	Val^5*O*	MeVal^{11}*O*	224	216	297	285	129	134	*3.4*

Table 5. *H-Bonds in Cyclosporin A from Different Calculations*[a]). d in pm, θ in °.

Donor (D)	Acceptor (A)	X-Ray				MDS1				MDNEW			
		d(D,A)	d(H,A)	θ(DH,A)	%	d(D,A)	d(H,A)	θ(DH,A)	%	d(D,A)	d(H,A)	θ(DH,A)	%
MeBmt^{1}O*H*	MeBmt^1*O*	–	–	–	–	282	211	128	*84*	316	251	122	*63*
MeBmt^{1}O*H*	MeLeu^9*O*[b])	279	186	167	*100*	–	–	–	–	–	–	–	–
Abu^{2}N*H*	Val^5*O*	284	184	171	*100*	310	221	150	*61*	299	212	145	*100*
Abu^{2}N*H*	MeVal^{11}*O*	–	–	–	–	302	230	129	*31*	339	274	123	*7*
Val^{5}N*H*	Abu^2*O*	302	207	154	*100*	300	207	157	*88*	288	192	161	*100*
Val^{5}N*H*	Sar^3*O*	–	–	–	–	–	–	–	–	341	273	126	*3*
Ala^{7}N*H*	Val^5*O*	–	–	–	–	299	231	125	*36*	293	216	133	*97*
Ala^{7}N*H*	MeVal^{11}*O*	298	196	162	*100*	306	212	159	*89*	294	224	126	*73*
D-Ala^{8}N*H*	MeLeu^6*O*	290	198	151	*100*	301	217	141	*69*	282	189	153	*100*

[a]) Only H-bonds with an occurrence greater 3% are displayed. The criterion is: the donor-H/acceptor angle θ(DH,A) must be larger than 90° and the donor-acceptor distance d(H,A) smaller than 0.25 nm.

[b]) Intermolecular H-bond to a neighbored molecule.

H-bonds is very similar to those observed in the crystal structure (*Table 5*). Although the MeBmt^1 side chain is folded over the backbone, it is still possible for the MeBmt^{1}O*H* to be involved in a H-bridge with the MeBmt^{1}C*O* as proposed in previous structural studies.

The average backbone dihedral angles and their rms fluctuations are given in *Table 6*. Cyclosporin A contains only four amide protons, and for the corresponding residues, it is possible to calculate the allowed values for the Φ angles from the J(N*H*,C(α)) values [42] obtained by NMR spectroscopy. The J's at low temperature and the corresponding Φ angles calculated with the *Karplus* equation are: Abu^2, $J_{exp} = 8.6$ Hz ($\Phi = -143$ and

Table 6. *Backbone Dihedral Angles* [°] *of Different Structures Cyclosporin A*[a])

Residue	X-Ray			MDS1			MDNEW		
	Φ	Ψ	ω	Φ	Ψ	ω	Φ	Ψ	ω
MeBmt[1]	−84	123	−175	−100(10.8)	95(11.0)	178 (6.7)	−89(3.2)	112(3.2)	169(1.9)
Abu[2]	−120	89	−178	−85(15.5)	97 (8.9)	−159 (8.6)	−97(3.7)	100(2.6)	176(2.4)
Sar[3]	73	−129	173	57 (9.6)	−116 (9.9)	169 (7.5)	79(4.2)	−108(5.3)	162(4.5)
MeLeu[4]	−99	21	180	−113 (9.6)	33(18.3)	176 (6.8)	−122(5.0)	30(4.3)	−174(3.1)
Val[5]	−112	126	167	−89(21.6)	120 (9.6)	180 (8.9)	−104(5.7)	123(2.7)	167(2.0)
MeLeu[6]	−90	99	−165	−90(11.0)	96(11.1)	−179 (6.1)	−82(2.2)	88(3.0)	178(1.9)
Ala[7]	−82	52	179	−90(14.2)	66(12.7)	178 (6.8)	−67(3.9)	54(3.4)	180(1.8)
D-Ala[8]	87	−124	−166	80(17.2)	−128(10.9)	−177 (7.4)	80(4.5)	−137(3.4)	−177(2.3)
MeLeu[9]	−119	99	−5	−132 (9.8)	113(13.0)	−11(15.0)	−125(2.2)	116(2.3)	−3(3.8)
MeLeu[10]	−138	64	−167	−121(11.4)	100(11.0)	−165(10.9)	−131(2.4)	86(3.7)	173(3.1)
MeVal[11]	−102	125	173	−123 (7.6)	104(11.5)	−172(11.9)	−120(2.9)	133(3.1)	154(1.9)

[a]) The numbers in brackets denote the rms fluctuation obtained by averaging.

−97°); Val[5], J_{exp} = 7.6 Hz (Φ = −150, −89, 72, and 47°); Ala[7], J_{exp} = 6.0 Hz (Φ = −161, −79, 90, and 30°); D-Ala[8], J_{exp} = 6.8 Hz (Φ = 156, 84, −83, and −37°). The values for the MDNEW structure (*Table 6*) are consistent with the experimentally determined values. The average dihedral angles in the loop region between Abu[2] and Val[15] are in agreement with the proposed angles for a βII′-turn [43] (see *Table 6*, Sar[3] = i + 1, MeLeu[4] = i + 2). The βII′-turn is also supported by the strong NOE observed between Sar[3]$H_{(pro\text{-}S)}$–C(α) and MeLeu[4]*Me*N, the visible NOE observed between Sar[3]$H_{(pro\text{-}S)}$–C(α) and Val[5]N*H* and the lack of a NOE between MeLeu[4]*Me*N and Sar[3]*Me*N. Sar[3]$H_{(pro\text{-}S)}$–C(α) lies in the plane of the C=O group of Sar[3] and consequently exhibits a strong downfield chemical shift as compared to the Sar[3]$H_{(pro\text{-}R)}$–C(α). Its configurational assignment is further supported by the existing NOE data.

A starting structure with a βI-turn in the calculation leads to an immediate flip of the amide bond to adopt the βII′-conformation (see previous section for details).

Flexibility and Fluctuations. – We are aware of the fact that the initial assumption of a rigid molecule in the determination of distances is in contradiction to the flexibility. This is especially true in light of recent results showing that the introduction of dynamic equilibria may considerably improve constrained MD simulations [44]. From this standpoint, we present here a static picture of a structure and hence, refinements or modifications can be obtained from more detailed studies of side-chain conformations. Experimental evidence can be obtained for χ_1, *i.e.* the C(α)–C(β) bond, from vicinal coupling constants. In case of an amino acid with 2 H–C(β), the combination of homo- and heteronuclear coupling constants can give an unequivocal population analysis under the assumption that only the three staggered rotamers are populated [5]. Based on the $^3J_{(H,H)}$ and $^3J_{(C,H)}$ values calculated for MeLeu[4] and MeLeu[6], the dominant conformations are with $\chi_1 = -60°$ and $\chi_1 = 180°$, respectively. This result is also the preferred conformation in MDNEW. For MeLeu[9], the most populated side-chain conformation calculated only from homonuclear $J(H\text{–}C(\alpha), H\text{–}C(\beta))$'s ($\chi_1 = -60°$) was also monitored during the MD simulation (*Table 7*).

The side chain of MeLeu[10] certainly can adopt more than one conformation. As described previously, the conformation about χ_1 in the crystal differs from the NOE-con-

Table 7. *Comparison of Calculated Side-Chain Populations and the Averaged χ_1 Angles from MDNEW*

	Coupling constants [Hz]		Population [%][a]			MDNEW
	$J(H-C(\alpha), H_{(pro-R)}-C(\beta))$	$J(H-C(\alpha), H_{(pro-S)}-C(\beta))$	$\chi_1 = -60°$	$\chi_1 = 180°$	$\chi_1 = +60°$	χ_1
MeLeu[4]	12.0	4.5	84	16	0	−151°
MeLeu[6]	6.0	10.5	30	70	0	−178°
MeLeu[9]	11.0	4.5	77	17	6	−60°
MeLeu[10]	8.0	6.5	49	35	16	−148°

[a]) The assignements of the rotamers are made from heteronuclear coupling constants measured by a hetero-E.COSY or by semiquantitative evaluation of COLOC spectra.

strained MD structure. This is also true for the MDNEW structure. The population analysis (*Table 7*) shows that even the sterically unfavored rotamer with $\chi_1 = 60°$ is considerably populated.

Flexibility certainly is also observed in the side chain of Abu[2]. As discussed previously, on the basis of the lack of larger chemical-shift nonequivalence of the $H-C(\beta)$'s, the NT_1 measurements, and the MD calculations, this side chain is not fixed at all [3]. This is again expressed in the variety of χ_1 values obtained from the different calculations (*Table 3*).

Even more flexibility is observed about bonds in side chains further away from the backbone. We have already pointed out the increasing mobility along the side chain of MeBmt[1] [3]. The NOE's from this side chain to the backbone and the new folding of this chain under the ring does not mean that it is fixed in one rotamer. Conformations with small distances are overemphasized in the structure due to the r^{-6} dependence of the NOE. Even only a relatively small amount of these conformations can express themselves clearly in NOE effects. Hence, in presenting a new structure in the form of a rigid picture, we only want to emphasize that this structure can contribute considerably to the conformational equilibrium and that this structure best represents the experimental data.

During the average period of 100 ps, no transitions of backbone dihedral angles in the turn region were observed. This supports the βII′-conformation shown in *Fig. 5*. The rms fluctuations of the C(α) atoms in the loop region are all small, in the range between 20 and 27 pm, some Φ and Ψ angle transitions are monitored. Hence, the loop region is more flexible than the turn region and the β-sheet. The most flexible dihedral angle is χ_3 of MeBmt[1]. This is supported by the increasing rms fluctuations of the MeBmt side-chain atoms.

Discussion. – With the larger number and more accurately determined distance restraints, we are able to distinguish between the βI- and βII′-turn: it is the βII′-turn. However, the most important fact of our new investigations is that the MeBmt side chain extends not towards the solvent, it is folded over the backbone, like in the crystal structure.

A new data set of distances was obtained from build-up rates of NOE at lower temperature. A good signal-to-noise ratio and the high resolution of the 600-MHz spectrum allowed to extract 117 distances. Although in this approach, the total relaxation matrix and conformational equilibria dynamics were not utilized, the results show a clear trend: the use of the extended data set drives the backbone of the molecule very close to

the X-ray structure (see *Table 6*). Almost all φ, Ψ, and ω angles now agree within the error limits. This is also found for the H-bonds of the four N*H*'s (*Table 5*). The only difference is in the intermolecular H-bond of MeBmtO*H* in the crystal which is obviously broken in solution. Now this group forms an intramolecular bond, as previously discussed. In addition, the γ-turn of Abu^{2}N*H*-MeVal^{11}*O* found in MDS1 has now disappeared, whereas a small population of a γ-turn Val^{5}N*H*-Sar^3*O* is observed, which is typical of a βII′-conformation [5].

Obviously, there are stronger deviations in the side-chain conformations. This was already discussed above, but it should be pointed out that despite the similar overall conformation, there are substantial differences in the χ torsions between the new structure and the X-ray.

In the recent literature, it was claimed that a βI-turn about Sar^3 and MeLeu^4 is also in agreement with our old data. This is only true when our previous MD calculations are not considered. However, the MD calculations always yielded a βII′-turn as the most stable solution conformation even for the old data set. It is clear from our new results that the βI-structure is not stable under the application of experimental NOE constraints. A small population of βI-turn conformation cannot be excluded in our methodology, and the presence of small populations of other conformations is always a possibility. It certainly depends on the definition of the term 'conformation'. It is known that a deviation of a few degrees in a bond angle normally costs only a negligible amount of energy. After all what we know about peptide conformation, it is not the flexibility but the relatively rigid conformation (but see the discussion in the previous chapter) which is surprising.

One might argue that the difference of the results presented here and the previous ones may be caused by different measuring conditions. Although this cannot be excluded, we think that the 50° lower measuring temperature and the relatively high concentration (83 mmol/l) cannot contribute so much to the difference. It might be that the entropy term destabilizes the folding of the MeBmt side chain at higher temperature, but this is difficult to prove because of the lack of exact data at higher temperatures.

Measurement Conditions. – 1. *500-MHz DQF-H,H-COSY Spectrum* (250 K): Sequence: D_1-90°-t_1-D_2-90°-t_2. Relaxation delay $D_1 = 1.5$ s, delay $D_2 = 3$ µs, 90° pulse 9.8 µs, acquisition time 430 ms, spectral width in F_1 and F_2 4761.90 Hz, size 4K, 32 acquisitions, 512 increments, quadrature detection in both dimensions, single zero filling in F_1 and apodization with a squared $\pi/3$-shifted sine bell in both dimensions.

2. *600-MHz NOESY Spectra* (252.5 K): Sequence: D_1-90° -t_1-90° -τ_{mix}-90°-t_2. Relaxation delay $D_1 = 1.5$ s, mixing time $\tau_{mix} = 80$, 120, 160, 200, 240, and 300 ms, 90° pulse 9.0 µs, acquisition time 340 ms, sweep width 6024.10 Hz in F_1 and F_2, 512 experiments in t_1, quadrature detection in both dimensions, zero filling up to 2 K in F_1 and apodization with a squared $\pi/2$-shifted sine bell in both dimensions. The integration was carried out with base-plane offset.

3. *600-MHz ROESY Spectrum* (250 K): Sequence: D_1-90°-t_1-spinlock-t_2. Relaxation delay $D_1 = 1.7$ s, mixing time 180 ms, sweep width 8196.72 Hz in F_1 and F_2, 56 acquisitions, 512 experiments in t_1, quadrature detection in both dimensions, zero filling up to 2 K in F_1 and apodization with a squared $\pi/2$-shifted sine bell in both dimensions.

We thank Dr. *Dale F. Mierke* for his careful reading of the manuscript. Financial support by the *Fond der Chemischen Industrie* and the *Deutsche Forschungsgemeinschaft* is gratefully acknowledged. *T. W.* and *M. K.* thank the *Fond der Chemischen Industrie* for fellowships.

REFERENCES

[1] H. Kessler, H.-R. Loosli, H. Oschkinat, in 'Peptides 1984', Proceedings of the 18th Eur. Pept. Symp., Ed. U. Ragnarsson, Almqvist and Wiksell Int., Stockholm, 1984, p. 65.

[2] H. Kessler, H.-R. Loosli, H. Oschkinat, *Helv. Chim. Acta* **1985**, *68*, 661.

[3] H.-R. Loosli, H. Kessler, H. Oschkinat, H.-P. Weber, T. J. Petcher, A. Widmer, *Helv. Chim. Acta* **1985**, *68*, 682.

[4] H. Kessler, H. Oschkinat, H.-R. Loosli, in 'Two-Dimensional NMR Spectroscopy', Eds. W. R. Croasmun and R. M. K. Carlson, Verlag Chemie, Weinheim, 1987, p. 259.

[5] H. Kessler, C. Griesinger, K. Wagner, *J. Am. Chem. Soc.* **1987**, *109*, 6927.

[6] J. Lautz, H. Kessler, J. M. Blaney, R. M. Scheek, W. F. van Gunsteren, *Int. J. Peptide Protein Res.* **1989**, *33*, 281.

[7] J. Lautz, H. Kessler, R. Kaptein, W. F. van Gunsteren, *J. Comput.-Aided Mol. Design* **1987**, *1*, 219.

[8] J. Lautz, H. Kessler, H. P. Weber, R. M. Wenger, W. F. van Gunsteren, *Biopolymers* **1990**, *29*, 1669.

[9] D. D. Beusen, G. R. Marshall, in 'Protein Structure and Engineering', Ed. O. Jardetzky, Plenum Press, New York – London, 1989, p. 97.

[10] D. D. Beusen, H. Iijima, G. R. Marshall, *Biochem. Pharmacol.* **1990**, *40*, 173.

[11] R. Pachter, R. B. Altman, J. Czaplicki, O. Jardetzky, *J. Magn. Reson.*, in press.

[12] A. Rüegger, M. Kuhn, H. Lichti, H.-R. Loosli, R. Huguenin, C. Quiquerez, A. von Wartburg, *Helv. Chim. Acta* **1976**, *59*, 1075.

[13] J. F. Borel, C. Feurer, H. U. Gubler, H. Stähelin, *Agents Actions* **1976**, *6*, 468.

[14] R. Traber, M. Kuhn, A. Rüegger, H. Lichti, H.-R. Loosli, A. von Wartburg, *Helv. Chim. Acta* **1977**, *60*, 1247.

[15] M. Dreyfuss, E. Härri, H. Hofmann, H. Kobel, W. Pache, H. Tscherter, *Eur. J. Appl. Microbiol.* **1976**, *3*, 125.

[16] R. M. Wenger, *Angew. Chem.* **1985**, *97*, 88.

[17] R. Traber, H. Hofmann, H.-R. Loosli, M. Ponelle, A. von Wartburg, *Helv. Chim. Acta* **1987**, *70*, 13.

[18] R. M. Wenger, *Helv. Chim. Acta* **1984**, *67*, 502.

[19] R. M. Wenger, *Sandorama* **1984**, *III*, 5.

[20] R. M. Wenger, *Helv. Chim. Acta* **1983**, *66*, 2308.

[21] R. M. Wenger, *Helv. Chim. Acta* **1983**, *66*, 2672.

[22] D. A. Evans, A. E. Weber, *J. Am. Chem. Soc.* **1986**, *108*, 6757.

[23] R. D. Tung, D. H. Rich, *Tetrahedron Lett.* **1987**, *28*, 1139.

[24] J. D. Aebi, M. K. Dhaon, D. H. Rich, *J. Org. Chem.* **1987**, *52*, 2881.

[25] U. Schmidt, W. Siegel, *Tetrahedron Lett.* **1987**, *28*, 2849.

[26] A. V. Rama Rao, T. G. Murali Dhar, T. K. Chakraborty, M. K. Gurjar, *Tetrahedron Lett.* **1988**, *29*, 2069.

[27] S. W. McCombie, B. B. Shankar, A. K. Ganguly, *Tetrahedron Lett.* **1989**, *30*, 7029.

[28] S. B. Park, G. P. Meier, *Tetrahedron Lett.* **1989**, *30*, 4215.

[29] A. V. Ramo Rao, T. G. Murali Dhar, D. Subhas Bose, T. K. Chakraborty, M. K. Gurjar, *Tetrahedron* **1989**, *45*, 7361.

[30] A. V. Ramo Rao, J. S. Yadaz, S. Chandrasekhar, C. Srinvias Rao, *Tetrahedron Lett.* **1989**, *30*, 6769.

[31] H. Oschkinat, Ph. D. thesis, Frankfurt, 1986.

[32] H. Kessler, M. Gehrke, J. Lautz, M. Köck, D. Seebach, A. Thaler, *Biochem. Pharmacol.* **1990**, *40*, 169.

[33] K. E. Miller, D. H. Rich, *J. Am. Chem. Soc.* **1989**, *111*, 8351.

[34] M. Gehrke, Ph. D. thesis, Frankfurt, 1989.

[35] M. J. Dellwo, A. J. Wand, *J. Am. Chem. Soc.* **1989**, *111*, 4571.

[36] D. G. Davis, A. Bax, *J. Magn. Reson.* **1985**, *64*, 533.

[37] H. Kessler, M. Gehrke, C. Griesinger, *Angew. Chem. Int. Ed.* **1988**, *27*, 490.

[38] T. L. James, B. A. Borgias, A. M. Bianucci, N. Jamin, N. Pattabiraman, E. Suzuki, N. Zhou, G. Zon, in 'NMR Spectroscopy in Drug Research', Eds. J. W. Jaroszewski, K. Schaumburg, and H. Kofod, Munksgaard, Copenhagen, 1988, p. 358.

[39] R. Boelens, T. M. G. Koning, R. Kaptein, *J. Mol. Struct.* **1988**, *173*, 299.

[40] R. Boelens, T. M. G. Koning, G. A. van der Marel, J. H. van Boom, R. Kaptein, *J. Magn. Reson.* **1989**, *82*, 290.

[41] J. Åquist, W. F. van Gunsteren, M. Leijonmark, O. Tupia, *J. Mol. Biol.* **1985**, *183*, 461.

[42] V. F. Bystrov, *Prog. Nucl. Magn. Reson. Spectrosc.* **1976**, *10*, 41.

[43] G. D. Rose, L. M. Gierasch, J. A. Smith, *Adv. Protein Chem.* **1985**, *37*, 1.

[44] H. Kessler, C. Griesinger, J. Lautz, A. Müller, W. F. van Gunsteren, H. J. C. Berendsen, *J. Am. Chem. Soc.* **1988**, *110*, 3393.